R-C^2: Cross-Modal Cycle Consistency Rewards Improve Multimodal Reasoning

Zirui Zhang[1] **Haoyu Dong**[2] **Kexin Pei**[3] **Chengzhi Mao**[1]
[1]Rutgers University [2]Columbia University [3]University of Chicago
`https://R-C2-cmlab.github.io/Cross-Modal-Cycle-Consistency-Rewards/`

Abstract

*Multimodal Large Language Models (MLLMs) suffer from a fundamental "modality gap," contradicting themselves on visual versus text views of the same content. This paper argues that this inconsistency is not a failure, but a powerful resource for self-reward multimodal learning. Instead of relying on flawed voting mechanisms that amplify systematic errors when the majority is wrong, we introduce cross-modal cycle consistency as rewards (*R-C^2*) to improve multimodal reasoning.* R-C^2 *performs backward inference from an answer to a query, switches modalities, and performs forward inference to verify the answer's consistency. This cycle serves as a dense, label-free reward that guides the model to resolve its own internal conflicts, while avoiding majority-is-wrong failures of standard voting methods. On standard benchmarks,* R-C^2 *mitigates modality-specific biases and improves reasoning accuracy by up to 7.6 points. Our results show that robust reasoning emerges not just from scaling data, but from achieving a bidirectional understanding of the multimodal world.*

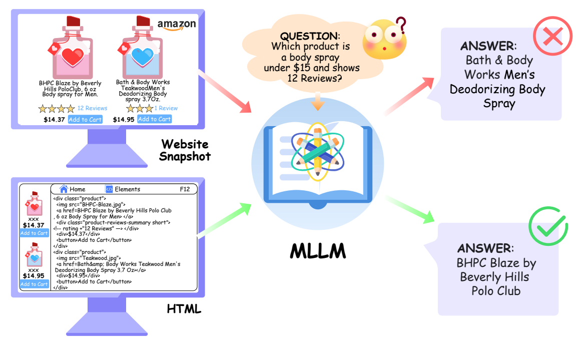

Figure 1. **Gap in Multimodal Reasoning.** Multimodal large language models (MLLMs) frequently fail the test of modal-invariance. For example, they produce conflicting answers for the same webpage when presented as a screenshot versus its raw HTML source. We introduce a cycle-consistency framework that directly targets this modality gap, leveraging the inconsistency itself as a signal to jointly improve reasoning and alignment.

1. Introduction

Multimodal Large Language Models (MLLMs) suffer from a fundamental modality gap [57], often contradicting themselves on visual versus text views of the same input content. As shown in Figure 1, we show that an MLLM can yield different answers for an identical webpage when presented as a screenshot versus its raw HTML source. As MLLMs are widely deployed in domains such as multimodal document understanding [30, 31], web UI navigation [18], and agentic systems [32, 48, 51], this lack of robustness and consistency can be a critical failure.

Most prior work attempts to improve reasoning through large-scale fine-tuning on meticulously curated datasets, which are expensive to construct and inherently limited in their ability to scale model performance [45]. Reinforcement learning (RL) [33, 34] offers an alternative, but hinges on reliable reward signals; unlike math [47, 54] or code [24, 37], complex multimodal answers are rarely verifiable. Without annotated query-answer pairs, recent self-improvement methods use majority voting [16, 43, 44]. However, these voting mechanisms suffer from inherent limitations. As illustrated in Figure 2, the problem is compounded in multimodal settings: when visual and textual predictions disagree—an extremely common scenario—the consensus becomes unstable and arbitrary. This leaves the underlying conflict unresolved and, in "majority-is-wrong" cases, actually amplifies the error.

Our key insight is that this cross-modal inconsistency is not a failure but a powerful, untapped resource for self-reward learning. Instead of relying on flawed voting, we introduce cross-modal cycle consistency (R-C^2), a framework that reframes this gap as a self-supervised reward signal. R-C^2 starts from a candidate answer. Then it performs backward inference to propose a query that would elicit that answer, then switches modalities to perform forward inference and reconstruct the original answer, as shown in Figure 3. This cycle serves as a dense, label-free reward that forces the model to resolve its own internal multimodal con-

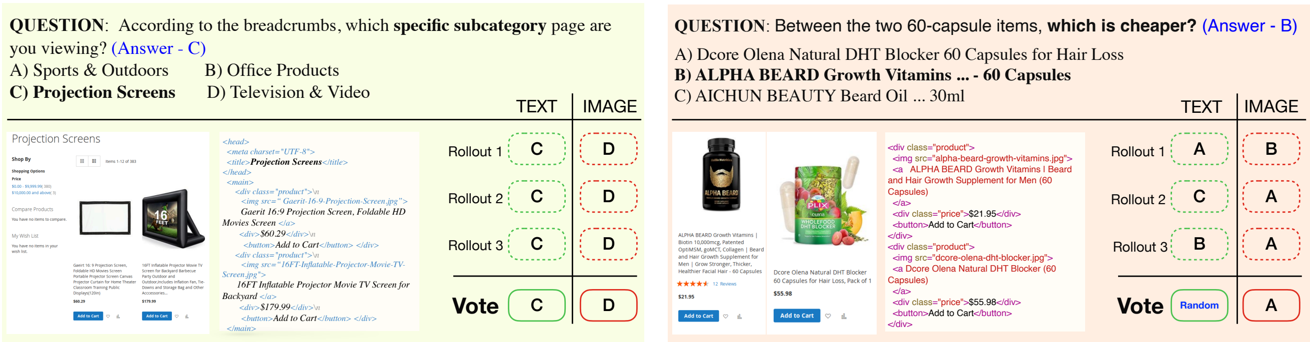

Figure 2. **Failure of multimodal voting.** *Left: Consistent Conflict* — both text and image modalities produce self-consistent predictions (*mode-stable*) but disagree with each other, and only one modality aligns with the ground truth. *Right: Unstable Recovery* — within a single modality, some rollouts yield the correct answer, but the majority vote remains wrong, reflecting intra-modal instability. Using multimodal voting can amplify biases or lose correct signals.

flicts, thus improving the reasoning capability.

Extensive experiments, complemented by a diverse suite of case-study visualizations that reveal modality conflicts and how R-C^2 resolves them, demonstrate that R-C^2 significantly improves multimodal reasoning capabilities without human annotations. In 3B and 8B multimodal LLMs, our method improves performance by up to 7.6 points on major multimodal benchmarks, including ScienceQA [26], ChartQA [29], InfoVQA [31], MathVista [27], A-OKVQA [35], and Visual Web Arena [18]. Moreover, our method greatly increases the consistency of cross-modal prediction. We further study the conditions under which our cross-modal cycle consistency approach provides the greatest benefit, offering insights into the nature of the modality gap in state-of-the-art models.

2. Related Work

Multimodal Large Language Models. Vision–language LLMs [23, 25, 39, 50] extend Language Models (LMs) [1–3, 40] with a vision encoder that maps images into the token (or embedding) space of the LM. In most systems, the vision encoder is pretrained separately and then frozen [39], and the supervision available for image–text is far sparser than for text-only corpora. These factors contribute to a *modality gap*: the same query can yield different answers depending on whether relevant information is provided as text or embedded in an image. Recent studies begin to characterize this gap [38, 52], but practical methods to close it remain limited. A prevailing strategy is to synthesize additional image–text QA pairs by first captioning images and then prompting an LM to generate query–answer pairs from the captions [5, 6, 10, 15, 23, 42, 56]; however, such pipelines often require nontrivial human curation and can propagate caption biases [11]. In contrast, we leverage incidental structure in naturally occurring multimodal data to improve understanding and reasoning without relying on large volumes of manually curated synthetic QA.

Reward Modeling. Reinforcement learning from human feedback (RLHF) and its extensions have been central to aligning LLMs with human preferences [14, 33]. For verifiable domains such as mathematics and code [19], outcome-based rewards are sufficient because correctness can be objectively measured. Beyond outcome-only supervision [36], recent work explores rewarding intermediate reasoning steps [12, 46, 49], often pairing process supervision with learned reward models that estimate the quality of partial solutions rather than final answers [21, 22, 28, 47]. Although these methods are effective in domains with verifiable feedback, they remain brittle in multimodal reasoning, where step-level evaluation is ambiguous, and learned reward models can inherit modality-specific biases. This leads to *reward misspecification*—overfitting to superficial textual or visual cues rather than genuine semantic correctness.

Label-Free Reinforcement Learning and Self-Evolution. To mitigate reliance on human or synthetic labels, recent trends pursue *label-free* self-improvement paradigms, including label-free RL [16], self-play [41], self-instruct [45], and self-training or self-refinement [13, 17, 58]. These methods iteratively generate and refine their own data using internal feedback, sometimes leveraging consistency or confidence as reward signals [22, 55, 59]. More advanced frameworks extend this idea to weak-to-strong learning [4, 20] and self-critique mechanisms [7, 8, 53], where models bootstrap improvement from self-generated critics. However, many systems still equate consensus with correctness, optimizing for agreement through majority voting [9]. This risks amplifying systematic biases, a phenomenon often described as a "majority-is-wrong" failure. In multimodal LLMs, this issue is exacerbated by *cross-modality inconsistency* [57], where visual and textual predictions diverge

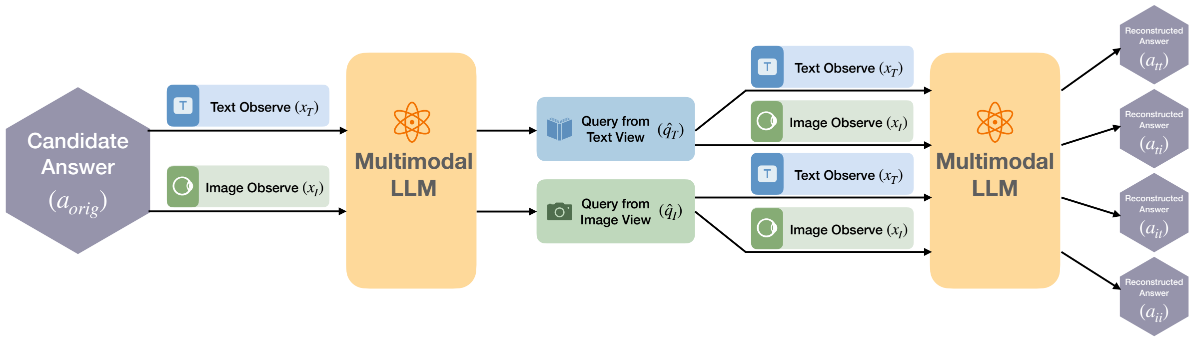

Figure 3. **Overview of multimodal cycle consistency.** Starting from a potential answer candidate a_{orig}, the model performs *backward inference* to reconstruct two latent queries, $\hat{q}_T$ from the text view x_T and $\hat{q}_I$ from the image view x_I. Each reconstructed query is then used for *forward inference* across both modalities, resulting in four reconstructed answers $\{a_{tt}, a_{ti}, a_{it}, a_{ii}\}$ generated via the paths $T \to T$, $T \to I$, $I \to T$, and $I \to I$. Cycle consistency is measured by whether the reconstructed answers remain consistent with the original a_{orig}, forming a full 4-way cross-modal reasoning cycle.

even when grounded in the same underlying content. Our method avoids voting through a cycle consistency.

3. Method

Our goal is to improve the multimodal reasoning capabilities of MLLM. We frame this as a reinforcement learning (RL) problem, where the key challenge is to acquire a reward signal without human labels. We first review self-rewarding methods based on consensus voting, showing how they fail in single-modal settings and how this failure is compounded in multimodal contexts. We then introduce our solution, R-C^2, a self-supervised reward framework that replaces flawed consensus with cross-modal cycle consistency.

3.1. The Failure of Consensus-Based Rewards

We define our MLLM as a model F_θ that produces an answer $\hat{\mathbf{a}}$ given a multimodal input $\mathbf{x}$ and a text query $\mathbf{q}$: $\hat{\mathbf{a}} = F_\theta(\mathbf{x}, \mathbf{q})$. The input $\mathbf{x}$ can be visual-only $\mathbf{x}_I$ (e.g., a screenshot), text-only $\mathbf{x}_T$ (e.g., HTML), or an interleaved mix $\mathbf{x}_M$.

To improve MLLM's reasoning capability, we follow the standard practice and optimize the model with reinforcement learning, a GRPO objective [36]. At each step, F_θ generates an answer for the query; a reward model assigns a scalar score, and we update θ to increase the likelihood of the sampled answer when the reward is high and decrease it when the reward is low. This aligns F_θ towards responses that consistently earn a higher reward. Formally, we will maximize this objective:

$$\mathcal{L}_{\text{GRPO}} = \mathbb{E}\left[\log \pi_\theta(\hat{\mathbf{a}}_i|\mathbf{x}_i, \mathbf{q}_i) \cdot \hat{A}(\hat{\mathbf{a}}_i, \mathbf{a}_i)\right]$$

where $A(\hat{a})$ is the advantage, which is calculated via

$$\hat{A}(\hat{\mathbf{a}}_i, \mathbf{a}_i) = \frac{r_i - \text{mean}(\mathbf{r})}{\text{std}(\mathbf{r})}, \tag{1}$$

where the advantage is calculated on the basis of its relative normalized value in the batch. This paradigm, however, hinges on a reliable reward function $r_i = R(\hat{\mathbf{a}}_i, \mathbf{a}_i)$ that requires a ground-truth answer $\mathbf{a}$ or an external verifier, both of which can be expensive to scale for many multimodal tasks.

Single-Modal Voting and "Majority-is-Wrong". To remove the need for labels, recent "self-improvement" methods like R^0 [16] generate their own rewards without labeled query-answer pairs. For a given text query, the model generates k candidate answers $\{\mathbf{a}_j\}_{j=1}^k$. Then it applies majority voting to select the most plausible answer $\mathbf{a}'$, which serves as a pseudo-label.

$$\mathbf{a}' = \text{mode}(\{\mathbf{a}_j\}_{j=1}^k).$$

It calculates the reward as $r_i = R(\hat{\mathbf{a}}_i, \mathbf{a}')$. The model is then trained to increase the probability of producing this majority-voted answer.

This approach suffers from a fundamental "majority-is-wrong" failure. If the model has a systematic bias, the majority of its answers will be incorrect. Voting will select an incorrect pseudo-label, and the RL objective will simply reinforce the model's own mistakes, leading to a collapse in performance.

Compounded Failure: Multimodal Voting. To extend voting to multimodal reasoning, we aggregate predictions from both the image and text modalities. For each query, the model answers k_I times from image views and k_T times from text views, predictions from the text modality $\{\mathbf{a}_t^T\}$ and the image modality $\{\mathbf{a}_j^I\}$ are pooled together, and the pseudo-label is determined by majority vote:

$$\mathbf{a}'_{\text{multi}} = \text{mode}\big(\{\mathbf{a}_j^I\}_{j=1}^{k_I} \cup \{\mathbf{a}_t^T\}_{t=1}^{k_T}\big).$$

The reward is then computed in the same way as the single-modal case, $r_i = R(\hat{\mathbf{a}}_i, \mathbf{a}'_{\text{multi}})$.

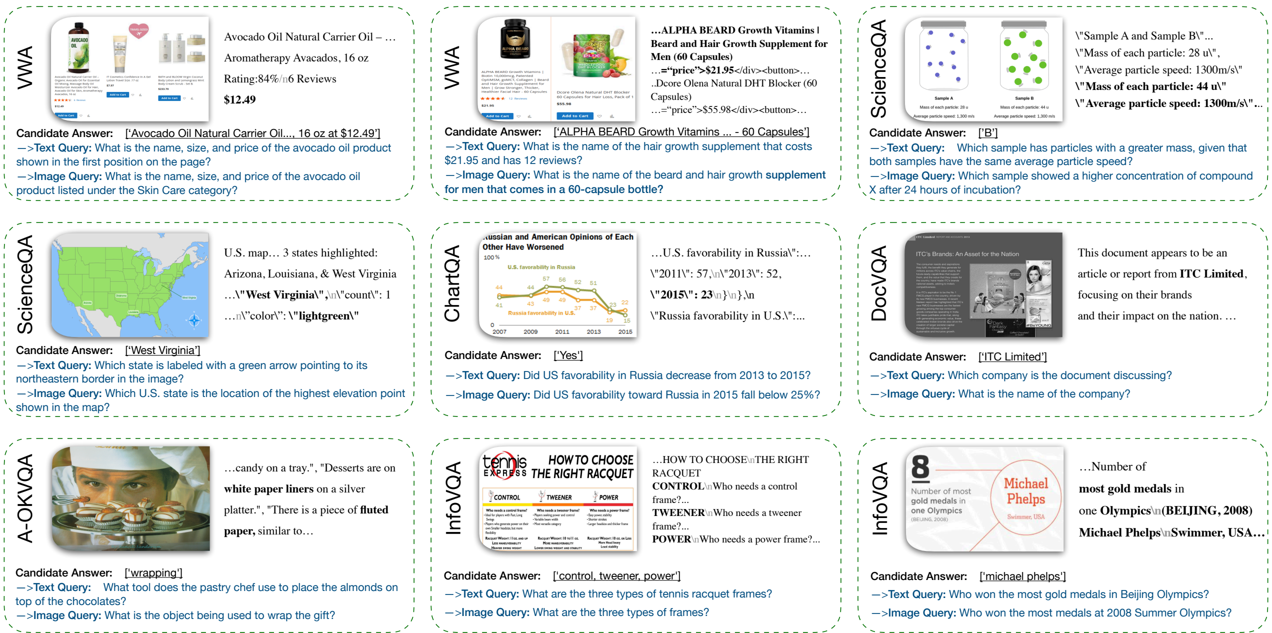

Figure 4. **Examples of the backward-inference (Answer→Query) step**. Given a Candidate Answer, the model generates distinct, semantically-grounded queries for both the text and image modalities. This demonstrates the viability of the first step of our cycle-consistency reward, enabling the model to check its answer in the alternate modality.

However, the problem of voting is compounded when applied to multimodal reasoning. A naive extension is to generate answers from different modalities and vote. However, we find that predictions from different modalities frequently disagree. As shown in Figure 2, when the model is presented with the same information in different forms (e.g., a chart image $\mathbf{x}_I$ vs. its data table $\mathbf{x}_T$), its answers often conflict. This cross-modal disagreement makes a simple majority vote unstable or arbitrary. If the visual and textual predictions differ, there is no clear consensus to follow, leaving the model without a reliable learning signal.

3.2. R-C^2: Self-Reward from Cycle Consistency

To break this cycle of self-reinforcing errors, we propose the Cross-Modal Cycle Consistency Reward (R-C^2). Our framework replaces flawed, unstable voting with a dense, self-supervised reward signal derived from the model's own internal consistency.

Our key insight is to shift from answer-side voting to answer-side verification. Instead of starting from a query to aggregate answers, we begin with a single candidate answer $\mathbf{a}_{\text{orig}}$—which may come from the model's own prediction or any available answer source, without relying on query–answer labels—and assess its logical self-consistency. To achieve this, MLLM first **backward infers** the probable queries that could elicit this answer $\mathbf{a}_{\text{orig}}$. This is achieved by conditioning on both $\mathbf{a}_{\text{orig}}$ and the content of one modality (e.g., text view $\mathbf{x}_T$), and prompting the MLLM to predict. This inferred query $\hat{q}$ is then fed back into the model, but this time conditioned on the *alternate* modality (e.g., image view $\mathbf{x}_I$), to **forward infer** a reconstructed answer, $\hat{\mathbf{a}}$. See Figure 4 for examples of the cycle consistency data. A binary reward is generated if the reconstructed $\hat{\mathbf{a}}$ is consistent with the original $\mathbf{a}_{\text{orig}}$:

$$r = \begin{cases} 1, & \text{if } \hat{\mathbf{a}} \text{ matches } \mathbf{a}_{\text{orig}}, \\ 0, & \text{otherwise.} \end{cases}$$

This self-verification design provides a reliable, self-supervised reward, eliminating the need for labeled query-answer pairs.

Multimodal Cycle Consistency. As shown in Figure 3, R-C^2 evaluates whether a candidate answer $\mathbf{a}_{\text{orig}}$ is stable by running a complete set of backward–forward cycles in both modalities. Given a sample with synchronized textual ($\mathbf{x}_T$) and visual ($\mathbf{x}_I$) views, we leverage both to form four distinct reasoning paths. First, in the **backward step**, the model infers two types of queries from $\mathbf{a}_{\text{orig}}$: $\hat{q}_T$ (conditioned on $\mathbf{x}_T$) and $\hat{q}_I$ (conditioned on $\mathbf{x}_I$). Next, in the **forward step**, each query is verified against both modalities. This results in four complete cycle directions:

$$T{\to}T, \quad T{\to}I, \quad I{\to}T, \quad I{\to}I.$$

Dataset	Qwen2.5-VL-3B-Instruct							
	Base Model		+ Voting (Text)		+ Voting (Image+Text)		+ R-C^2 (Ours)	
	Text Acc	Vision Acc	Text Acc	Vision Acc	Text Acc	Vision Acc	Text Acc	Vision Acc
ScienceQA	68.9	76.0	70.7 (+1.8)	76.2 (+0.2)	73.1 (+4.2)	78.0 (+2.0)	**76.7 (+7.8)**	**83.3 (+7.3)**
ChartQA	71.1	82.8	76.0 (+4.9)	83.6 (+0.8)	76.2 (+5.1)	83.5 (+0.7)	**77.2 (+6.1)**	**84.8 (+2.0)**
MathVista	49.8	64.8	50.6 (+0.8)	65.0 (+0.2)	52.1 (+2.3)	65.7 (+0.9)	**55.8 (+6.0)**	**67.6 (+2.8)**
VWA	69.0	62.9	**74.5 (+5.5)**	63.1 (+0.2)	73.3 (+4.3)	64.5 (+1.6)	**74.5 (+5.5)**	**67.1 (+4.2)**
A-OKVQA	70.3	86.1	73.9 (+3.6)	87.6 (+1.5)	74.2 (+3.9)	87.7 (+1.6)	**75.2 (+4.9)**	**88.8 (+2.7)**
DocVQA	74.7	90.0	76.2 (+1.5)	90.3 (+0.3)	76.4 (+1.7)	**90.4 (+0.4)**	**76.6 (+1.9)**	90.3 (+0.3)
InfoVQA	54.9	74.1	55.6 (+0.7)	74.2 (+0.1)	56.1 (+1.2)	**74.3 (+0.2)**	**56.3 (+1.4)**	**74.3 (+0.2)**
Average	65.5	76.7	68.2 (+2.7)	77.1 (+0.4)	68.8 (+3.3)	77.7 (+1.0)	**70.3 (+4.8)**	**79.5 (+2.8)**
Dataset	**Qwen3-VL-8B-Instruct**							
	Base Model		**+ Voting (Text)**		**+ Voting (Image+Text)**		**+ R-C^2 (Ours)**	
	Text Acc	Vision Acc	Text Acc	Vision Acc	Text Acc	Vision Acc	Text Acc	Vision Acc
ScienceQA	72.9	90.3	72.6 (-0.3)	90.0 (-0.3)	74.8 (+1.9)	90.0 (-0.3)	**75.9 (+3.0)**	**91.3 (+1.0)**
ChartQA	78.8	85.1	80.2 (+1.4)	85.3 (+0.2)	80.2 (+1.4)	85.8 (+0.7)	**80.8 (+2.0)**	**86.0 (+0.9)**
MathVista	62.0	73.8	61.8 (-0.2)	73.7 (-0.1)	64.8 (+2.8)	76.5 (+2.7)	**66.3 (+4.3)**	**76.9 (+3.1)**
VWA	84.3	81.2	85.1 (+0.8)	81.6 (+0.4)	85.3 (+1.0)	81.0 (-0.2)	**85.7 (+1.4)**	**81.8 (+0.6)**
A-OKVQA	72.2	86.4	72.8 (+0.6)	86.8 (+0.4)	73.4 (+1.2)	86.9 (**+0.5**)	**73.5 (+1.3)**	**87.3 (+0.9)**
DocVQA	78.0	92.9	79.2 (+1.2)	93.6 (+0.7)	**79.4 (+1.4)**	**93.8 (+0.9)**	**79.4 (+1.4)**	93.3 (+0.4)
InfoVQA	60.4	82.6	60.7 (+0.3)	82.5 (-0.1)	61.9 (+1.5)	83.1 (+0.5)	**62.7 (+2.3)**	**83.3 (+0.7)**
Average	72.7	84.6	73.2 (+0.5)	84.8 (+0.2)	74.3 (+1.6)	85.3 (+0.7)	**74.9 (+2.2)**	**85.7 (+1.1)**

Table 1. **Multimodal Reasoning Accuracy.** We compare the Base Model, Voting (Text-only), Voting (Image+Text), and our R-C^2-RL method on Qwen2.5-VL-3B-Instruct (top) and Qwen3-VL-8B-Instruct (bottom). Each cell reports Text Accuracy (input content in text format) and Vision Accuracy (input content in image format), with green numbers indicating absolute improvements of R-C^2 over the base model. We **bold** the best accuracy for each dataset. Multimodal voting consistently outperforms text-only voting and the base model, and R-C^2 achieves the largest gains across nearly all benchmarks.

Dataset	Qwen2.5-VL-3B				Qwen3-VL-8B			
	Base	Voting (Text)	Voting (Image+Text)	R-C^2 (Ours)	Base	Voting (Text)	Voting (Image+Text)	R-C^2 (Ours)
ScienceQA	74.9	79.7 (+4.8)	81.7 (+6.8)	**84.9 (+10.0)**	74.7	75.3 (+0.6)	77.3 (+2.6)	**78.3 (+3.6)**
ChartQA	73.4	79.2 (+5.8)	78.9 (+5.5)	**79.5 (+6.1)**	81.4	82.7 (+1.3)	83.2 (+1.8)	**83.5 (+2.1)**
MathVista	57.3	58.8 (+1.5)	59.2 (+1.9)	**61.4 (+4.1)**	64.7	64.8 (+0.1)	69.0 (+4.3)	**69.2 (+4.5)**
VWA	63.9	66.9 (+3.0)	**70.0 (+6.1)**	67.1 (+3.2)	79.2	80.0 (+0.8)	79.8 (+0.6)	**81.2 (+2.0)**
A-OKVQA	67.8	80.1 (+12.3)	80.2 (+12.4)	**80.3 (+12.5)**	70.2	79.3 (+9.1)	**80.3 (+10.1)**	79.6 (+9.4)
DocVQA	75.2	76.9 (+1.7)	**77.1 (+1.9)**	76.6 (+1.4)	79.2	79.9 (+0.7)	**80.0 (+0.8)**	**80.0 (+0.8)**
InfoVQA	56.5	56.9 (+0.4)	57.8 (+1.3)	**58.5 (+2.0)**	60.9	61.1 (+0.2)	62.1 (+1.2)	**65.8 (+4.9)**
Average	67.0	71.2 (+4.2)	72.1 (+5.1)	**72.6 (+5.6)**	72.9	74.7 (+1.8)	76.0 (+3.1)	**76.8(+3.9)**

Table 2. **Multimodal Consistency Ratio.** We compare both Qwen2.5-VL-3B and Qwen3-VL-8B. Each dataset is evaluated under four supervision settings: Base, +Voting (Text), +Voting (Image+Text), and +R-C^2. Values in (green) indicate absolute improvements of R-C^2 over the base model. Across most datasets, R-C^2 achieves the highest cross-modal agreement.

A reward is generated for each path where every $a \in \{a_{tt}, a_{ii}, a_{ti}, a_{it}\}$ matches $\mathbf{a}_{\text{orig}}$. Crucially, R-C^2 uses all four cycles. Same-modality cycles ($T \to T$, $I \to I$) enforce internal stability. Cross-modality cycles ($T \to I$, $I \to T$) force the model to **resolve its modality gap** and align semantics. This full 4-way evaluation provides a comprehensive signal, demanding both intra-modal robustness and cross-modal agreement.

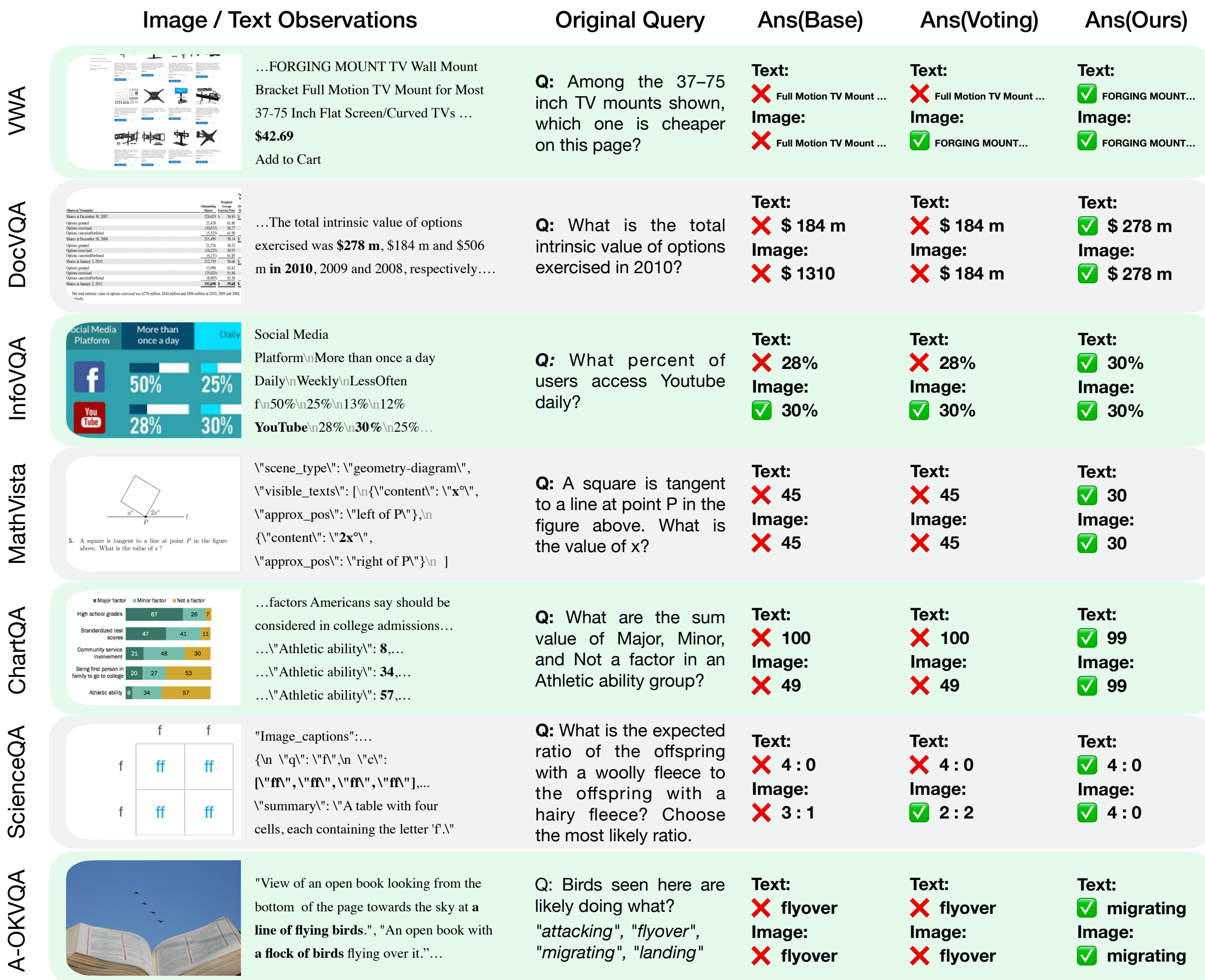

Figure 5. **Visual comparison among the base model, voting baseline, and R-C^2 (ours).** For each example, we display the original multimodal observation, the query, and the predictions from text and image modalities under different methods. The base model and voting baseline often yield either conflicting answers across modalities or spurious agreements on incorrect predictions, reflecting the modality gap and unreliable consensus confidence. In contrast, R-C^2 enforces cycle-based alignment, producing answers that are both correct and consistent across modalities.

Training Pipeline. While we can do this cross-modal cycle consistency online, which means we dynamically generate new cycle data using the model updated from the previous step, we adopt an offline strategy, which pre-generates the entire synthetic cycle dataset before training begins. While the online method allows the data to co-evolve with the model, we find the offline version is substantially more training-efficient, as it permits the pre-computation and batching of all cycle data. Our full pipeline proceeds in three stages: (0) an optional step for multimodal data preparation, followed by our core two-stage algorithm: (1) constructing cycles from candidate answers and (2) reinforcement learning with cycle rewards.

(0) Multimodal data preparation. Each training sample provides semantically aligned visual and textual views. For datasets that naturally contain both modalities (e.g., webpages and their corresponding HTML), we directly use the paired image-text inputs. For image-only datasets, we obtain the textual view by prompting the MLLM we use to generate a reliable semantic description. This ensures that every sample contains a coherent multimodal representation suitable for cross-modal cycles.

(1) Constructing cycles from candidate answers. Training begins by sampling one or more *candidate answers* from the model's current policy using either the image or the text modality. Each candidate answer is then used to infer a

backward query through the same MLLM model. The resulting $(\hat{q}, a_{\text{orig}})$ pair forms a synthetic query–answer pair that reflects the model's internal reasoning. These pairs serve as the data for cycle verification and provide self-generated supervision without requiring labeled QA data.

(2) Reinforcement learning with cycle rewards. Given the backward query, the model performs a forward pass (in the same or alternate modality) to obtain a reconstructed answer. Comparing this answer with the original one yields the binary cycle-consistency reward for GRPO training.

4. Experiments

4.1. Baselines

We use Qwen2.5-VL-3B-Instruct and Qwen3-VL-8B-Instruct as the baseline. We also adopt R0's [16] majority voting as our baseline: for each query, the model generates multiple rollouts and adopts the most frequent answer as the pseudo-label. In the text-only case, voting is applied over textual rollouts, while in the multimodal setting, predictions from image and text rollouts are pooled together and voted jointly. Unless otherwise stated, we set the number of rollouts to 4 per modality in all voting-based experiments. See Sec. 3.1 for procedural details.

4.2. Implementation Details

We train all models using the GRPO objective with a learning rate of $1e-6$. Experiments are conducted on 4 Blackwell 6000 Pro GPUs with mixed-precision training. For each update step, the model samples four rollouts per modality using a temperature of 1.0 and a top-p of 0.95. We use an effective batch size of 256 for VWA, InfoVQA, and DocVQA (long-input datasets), and 1024 for all other datasets, via gradient accumulation. Larger batch sizes are adopted when GPU memory permits, and training is run for up to 100 steps. We use a validation set for model selection and early stopping.

4.3. Datasets

We evaluate R-C^2 across six multimodal reasoning benchmarks spanning diverse visual–textual understanding tasks. *ScienceQA* [26] covers general visual question answering; *ChartQA* [29] focuses on reasoning over data visualizations; *DocVQA* [30], *InfoVQA* [31] emphasize OCR-based reasoning in infographic-style images; *A-OKVQA* [35] extends VQA into open-domain reasoning over natural images, requiring commonsense and factual knowledge beyond visual perception; and *MathVista* [27] evaluates visual mathematical reasoning grounded in figures and quantitative relations. We additionally repurpose the *VWA* benchmark [18] to assess reasoning in complex web environments. Specifically, we use its *shopping website* subset and use multiple-choice question–answer pairs to enable consistent and straightforward evaluation.

Cycle Type	ScienceQA			ChartQA		
	Text	Vision	Cons.	Text	Vision	Cons.
Single	74.0	81.7	81.2	76.2	83.7	77.3
Cross	75.8	80.1	83.1	76.5	83.8	78.4
Mixed	76.7	83.3	84.9	77.2	84.8	79.5

Table 3. Ablation of cycle path configurations in R-C^2 on ScienceQA and ChartQA using Qwen2.5-VL-3B-Instruct. *Single* uses intra-modal cycles (I→I, T→T); *Cross* uses cross-modal cycles (I→T, T→I); *Mixed* combines all four paths. The mixed configuration yields the highest accuracy and consistency.

4.4. Main Results

Table 1 and Table 2 summarize the overall performance of R-C^2 across six multimodal reasoning benchmarks using the Qwen2.5-VL-3B-Instruct and Qwen3-VL-8B-Instruct models. We compare our method against the majority vote–based self-improvement method, which for single-modality voting we denote as *Voting (Text-only)*, and for multimodal voting we denote as *Voting (Image+Text)*.

As shown in Table 1, R-C^2 consistently outperforms all voting baselines across datasets and model scales. On ScienceQA, our method improves text and vision accuracy by up to (+7.8/+7.3) points (Qwen2.5-VL-3B) and (+3.0/+1.0) points (Qwen3-VL-8B). Comparable gains appear on ChartQA (+6.1/+2.0) points, MathVista (+6.0/+2.8) points and A-OKVQA (+4.9/+2.7) points, while the complex VWA benchmark sees substantial improvements of (+5.5/+4.2) points. This trend holds on DocVQA and InfoVQA, confirming the cross-modal reward benefits for both modalities.

Our accuracy gain stems from addressing a fundamental flaw in voting baselines. While single modal aggregation improves on the baseline, it fails to model inter-modal relationships. An erroneous rollout can dominate the vote, and even multimodal voting is insufficient in fixing it: it is common that modalities disagree, and the vote simply collapses to the dominant modality. This leaves the underlying conflict unresolved and injects substantial noise into the training signal, limiting accuracy. In contrast, R-C^2 enforces both finer-grained within-modality and cross-modal consistency. The cycles stabilize unstable reasoning steps and, crucially, resolve inter-modal conflicts, leading to a direct and significant improvement in reasoning capability.

Moreover, Table 2 reports the Consistency Ratio—the proportion of samples for which image- and text-based predictions agree. R-C^2 substantially increases agreement across all benchmarks, reaching up to +12.5 points on A-OKVQA, +10.0 points on ScienceQA and +6.1 points on

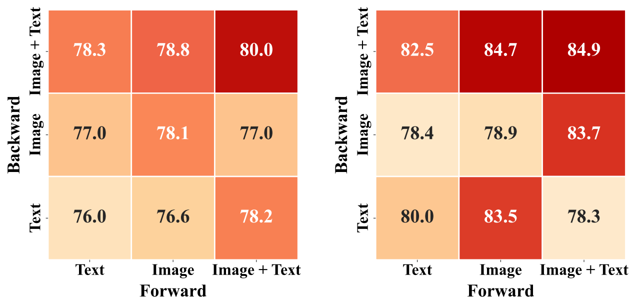

(a) Average accuracy across image and text modalities (%).

(b) Cross-modal predictions consistency ratio (%).

Figure 6. **Importance of cross modal in cycle consistency path.** We show ScienceQA results under R-C^2 training with nine different forward–backward cycle paths. Backward denotes *answer* $\rightarrow$ *query* and forward denotes *query* $\rightarrow$ *answer* The heatmaps show (a) average accuracy and (b) cross-modal consistency across all modality configurations. Using both image and text modalities for backward query generation consistently leads to higher accuracy and stronger cross-modal agreement, suggesting that multimodal grounding provides a more reliable signal for cycle-consistent reasoning.

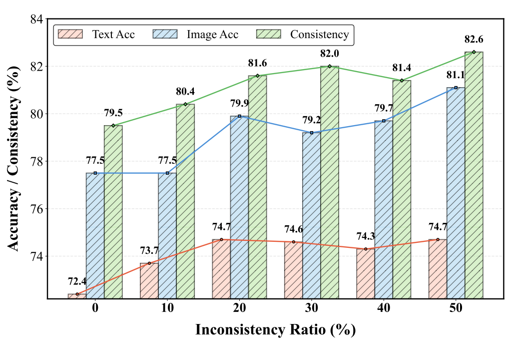

Figure 7. **Effect of cross-modal inconsistency ratio on ScienceQA performance.** We fine-tune Qwen2.5-VL-3B-Instruct on ScienceQA with varying fractions of cross-modal inconsistent training samples. As the inconsistency ratio increases from 0% to 50%, both answer accuracy and cross-modal consistency systematically improve. This suggests that exposing the model to more modality conflicts provides a useful structural signal for the RL objective, enabling it to better resolve cross-modal disagreements and yielding more stable multimodal reasoning.

ChartQA with Qwen2.5-VL-3B. For the larger Qwen3-VL-8B model, consistency continues to improve (+3–5) points, indicating that R-C^2 complements model scaling and remains effective even as baseline accuracy increases. The gains suggest that enforcing cross-modal cycle consistency not only improves accuracy but also stabilizes multimodal reasoning by aligning both modalities toward a shared semantic interpretation, making the model more robust.

4.5. Analysis

We conduct a series of ablation studies to better understand how each design choice affects the performance of **R-C^2**. Our analyses cover cycle path strategies, how multi-modal inconsistency data affects model reasoning ability, and how to retrieve candidate answers.

Importance of Multimodal Interaction. We conduct an ablation study to isolate the impact of multimodal interaction. In Table 3, we compare three training configurations: 1) single-modality cycle consistency (*Single*), 2) cross-modality cycle consistency (*Cross*), and 3) a combination of both (*Mixed*). Our results show that introducing cross-modal interaction consistently outperforms the single-modality baseline. Moreover, the two objectives prove to be complementary: the *Mixed* variant yields a significant accuracy gain over using either in isolation. Consequently, we adopt the *Mixed* configuration for all subsequent experiments.

Ablation Study of Cycle Paths. We analyze the contribution of specific cycle paths in Figure 6. We report accuracy and consistency across a grid where rows indicate the query-generation modality and columns indicate the answer-prediction modality. The "Image + Text" entries represent the joint use of both modalities. We observe that single-path supervision is insufficient; configurations restricted to one path (e.g., only Image$\rightarrow$Image) result in the lowest performance. In contrast, incorporating cross-modal paths (e.g., Text$\rightarrow$Image) significantly improves consistency by forcing the model to align semantic representations across modalities. Ultimately, the best performance is achieved by the full union of all paths (bottom-right cell). This confirms that maximizing the diversity of cycle constraints provides the most robust supervision, effectively mitigating shortcuts and grounding the model's reasoning.

The Importance of Cross-Modal Disagreement Data for Training. We investigate whether training on conflicting data helps or hinders learning. We construct controlled ScienceQA subsets (3.2k samples) with fixed size but varying rates of cross-modal inconsistency ($\{0\%, \ldots, 50\%\}$). Figure 7 shows that as the inconsistency ratio increases, both accuracy and consistency improve. This indicates that conflicting samples serve as effective "hard examples." By forcing the model to resolve these disagreements via the cycle reward, the RL process achieves tighter cross-modal alignment and more robust reasoning than when training on easy, consistent data.

Source of Candidate Answers. We further study how the choice of candidate answers used to start the cycle affects final performance. We compare two ways of obtaining the candidate answer: (1) *Self-generated answer*, where the MLLM predicts an initial answer from the input (fully self-supervised), and (2) *Training-set answer*, where we directly

Source of Candidate	A-OKVQA			VWA		
	Vision Acc	Text Acc	Cons.	Vision Acc	Text Acc	Cons.
Base model	86.1	70.3	67.8	69.0	62.9	63.9
Self-generated answer	87.3	71.6	77.6	74.9	65.3	68.2
Training set answer	88.8	75.2	80.3	74.5	67.1	67.1

Table 4. **Effect of candidate answer source for initiating the cycle**. We compare using the model's own predicted answer (*Self-generated*) versus using the reference answer from the dataset (*Training-set answer*). Results show comparable or better performance without requiring annotated QA pairs, highlighting the self-bootstrapping capability of R-C^2.

use the reference answer from the dataset (without relying on a labeled query–answer pair). Both settings are scalable because neither requires human annotation of queries nor majority-vote pseudo labels.

As shown in Table 4, the self-generated setting achieves performance nearly identical to the training-set answer setting on web understanding tasks. This demonstrates that R-C^2 can reliably bootstrap its own supervision without externally provided answers, highlighting strong potential for scalable, label-free multimodal reinforcement learning.

5. Conclusion

Our work shows that robust multimodal reasoning requires models to achieve a rigorous, bidirectional alignment between modalities. We start from a key failure in this area—a modality gap where MLLMs contradict themselves on visual versus textual views of the same content. Instead of merely aggregating conflicting votes, our framework, R-C^2, exploits this gap via a cross-modal cycle, which is a powerful untapped resource for self-reward learning. R-C^2 performs backward inference to hypothesize a query, switches modalities, and performs forward inference to reconstruct the answer. By teaching the model to resolve its own internal conflicts, R-C^2 leads to substantial improvements in both reasoning accuracy and cross-modal alignment. Our work suggests that the next generation of robust multimodal reasoning will emerge not just from scaling data, but from enforcing a more rigorous, bidirectional understanding of the world.

Acknowledgment

This work used Purdue Anvil GPU through allocation 250774 from the Advanced Cyberinfrastructure Coordination Ecosystem: Services & Support (ACCESS) program, which is supported by U.S. National Science Foundation grants 2138259, 2138286, 2138307, 2137603, and 2138296. We thank Guangxing Han for the insightful discussion.

References

[1] Josh Achiam, Steven Adler, Sandhini Agarwal, Lama Ahmad, Ilge Akkaya, Florencia Leoni Aleman, Diogo Almeida, Janko Altenschmidt, Sam Altman, Shyamal Anadkat, et al. Gpt-4 technical report. *arXiv preprint arXiv:2303.08774*, 2023. 2

[2] Jinze Bai, Shuai Bai, Yunfei Chu, Zeyu Cui, Kai Dang, Xiaodong Deng, Yang Fan, Wenbin Ge, Yu Han, Fei Huang, et al. Qwen technical report. *arXiv preprint arXiv:2309.16609*, 2023.

[3] Tom Brown, Benjamin Mann, Nick Ryder, Melanie Subbiah, Jared D Kaplan, Prafulla Dhariwal, Arvind Neelakantan, Pranav Shyam, Girish Sastry, Amanda Askell, et al. Language models are few-shot learners. *Advances in neural information processing systems*, 33:1877–1901, 2020. 2

[4] Collin Burns, Pavel Izmailov, Jan Hendrik Kirchner, Bowen Baker, Leo Gao, Leopold Aschenbrenner, Yining Chen, Adrien Ecoffet, Manas Joglekar, Jan Leike, et al. Weak-to-strong generalization: Eliciting strong capabilities with weak supervision. *arXiv preprint arXiv:2312.09390*, 2023. 2

[5] Paola Cascante-Bonilla, Hui Wu, Letao Wang, Rogerio S Feris, and Vicente Ordonez. Simvqa: Exploring simulated environments for visual question answering. In *Proceedings of the IEEE/CVF conference on computer vision and pattern recognition*, pages 5056–5066, 2022. 2

[6] Feilong Chen, Minglun Han, Haozhi Zhao, Qingyang Zhang, Jing Shi, Shuang Xu, and Bo Xu. X-llm: Bootstrapping advanced large language models by treating multi-modalities as foreign languages. *arXiv preprint arXiv:2305.04160*, 2023. 2

[7] Jiaqi Chen, Bang Zhang, Ruotian Ma, Peisong Wang, Xiaodan Liang, Zhaopeng Tu, Xiaolong Li, and Kwan-Yee K Wong. Spc: Evolving self-play critic via adversarial games for llm reasoning. *arXiv preprint arXiv:2504.19162*, 2025. 2

[8] Zixiang Chen, Yihe Deng, Huizhuo Yuan, Kaixuan Ji, and Quanquan Gu. Self-play fine-tuning converts weak language models to strong language models. *arXiv preprint arXiv:2401.01335*, 2024. 2

[9] Zhipeng Chen, Xiaobo Qin, Youbin Wu, Yue Ling, Qinghao Ye, Wayne Xin Zhao, and Guang Shi. Pass@ k training for adaptively balancing exploration and exploitation of large reasoning models. *arXiv preprint arXiv:2508.10751*, 2025. 2

[10] Wenliang Dai, Junnan Li, Dongxu Li, Anthony Tiong, Junqi Zhao, Weisheng Wang, Boyang Li, Pascale N Fung, and

Steven Hoi. Instructblip: Towards general-purpose vision-language models with instruction tuning. *Advances in neural information processing systems*, 36:49250–49267, 2023. 2

[11] Sivan Doveh, Assaf Arbelle, Sivan Harary, Roei Herzig, Donghyun Kim, Paola Cascante-Bonilla, Amit Alfassy, Rameswar Panda, Raja Giryes, Rogerio Feris, et al. Dense and aligned captions (dac) promote compositional reasoning in vl models. *Advances in Neural Information Processing Systems*, 36:76137–76150, 2023. 2

[12] Guhao Feng, Bohang Zhang, Yuntian Gu, Haotian Ye, Di He, and Liwei Wang. Towards revealing the mystery behind chain of thought: a theoretical perspective. *Advances in Neural Information Processing Systems*, 36:70757–70798, 2023. 2

[13] Caglar Gulcehre, Tom Le Paine, Srivatsan Srinivasan, Ksenia Konyushkova, Lotte Weerts, Abhishek Sharma, Aditya Siddhant, Alex Ahern, Miaosen Wang, Chenjie Gu, et al. Reinforced self-training (rest) for language modeling. *arXiv preprint arXiv:2308.08998*, 2023. 2

[14] Daya Guo, Dejian Yang, Haowei Zhang, Junxiao Song, Ruoyu Zhang, Runxin Xu, Qihao Zhu, Shirong Ma, Peiyi Wang, Xiao Bi, et al. Deepseek-r1: Incentivizing reasoning capability in llms via reinforcement learning. *arXiv preprint arXiv:2501.12948*, 2025. 2

[15] Vipul Gupta, Zhuowan Li, Adam Kortylewski, Chenyu Zhang, Yingwei Li, and Alan Yuille. Swapmix: Diagnosing and regularizing the over-reliance on visual context in visual question answering. In *Proceedings of the IEEE/CVF conference on computer vision and pattern recognition*, pages 5078–5088, 2022. 2

[16] Chengsong Huang, Wenhao Yu, Xiaoyang Wang, Hongming Zhang, Zongxia Li, Ruosen Li, Jiaxin Huang, Haitao Mi, and Dong Yu. R-zero: Self-evolving reasoning llm from zero data. *arXiv preprint arXiv:2508.05004*, 2025. 1, 2, 3, 7

[17] Jiaxin Huang, Shixiang Shane Gu, Le Hou, Yuexin Wu, Xuezhi Wang, Hongkun Yu, and Jiawei Han. Large language models can self-improve. *arXiv preprint arXiv:2210.11610*, 2022. 2

[18] Jing Yu Koh, Robert Lo, Lawrence Jang, Vikram Duvvur, Ming Lim, Po-Yu Huang, Graham Neubig, Shuyan Zhou, Russ Salakhutdinov, and Daniel Fried. Visualwebarena: Evaluating multimodal agents on realistic visual web tasks. In *Proceedings of the 62nd Annual Meeting of the Association for Computational Linguistics (Volume 1: Long Papers)*, pages 881–905, 2024. 1, 2, 7

[19] Nathan Lambert, Jacob Morrison, Valentina Pyatkin, Shengyi Huang, Hamish Ivison, Faeze Brahman, Lester James V Miranda, Alisa Liu, Nouha Dziri, Shane Lyu, et al. Tulu 3: Pushing frontiers in open language model post-training. *arXiv preprint arXiv:2411.15124*, 2024. 2

[20] Jan Leike and Ilya Sutskever. Introducing superalignment, 2023. OpenAI Blog. 2

[21] Ruosen Li, Ziming Luo, and Xinya Du. Fg-prm: Fine-grained hallucination detection and mitigation in language model mathematical reasoning. *arXiv preprint arXiv:2410.06304*, 2024. 2

[22] Zongxia Li, Yapei Chang, Yuhang Zhou, Xiyang Wu, Zichao Liang, Yoo Yeon Sung, and Jordan Lee Boyd-Graber. Semantically-aware rewards for open-ended r1 training in free-form generation. *arXiv preprint arXiv:2506.15068*, 2025. 2

[23] Haotian Liu, Chunyuan Li, Qingyang Wu, and Yong Jae Lee. Visual instruction tuning. *Advances in neural information processing systems*, 36:34892–34916, 2023. 2

[24] Jiawei Liu and Lingming Zhang. Code-r1: Reproducing r1 for code with reliable rewards. *arXiv preprint arXiv:2503.18470*, 3, 2025. 1

[25] Haoyu Lu, Wen Liu, Bo Zhang, Bingxuan Wang, Kai Dong, Bo Liu, Jingxiang Sun, Tongzheng Ren, Zhuoshu Li, Hao Yang, et al. Deepseek-vl: towards real-world vision-language understanding. *arXiv preprint arXiv:2403.05525*, 2024. 2

[26] Pan Lu, Swaroop Mishra, Tanglin Xia, Liang Qiu, Kai-Wei Chang, Song-Chun Zhu, Oyvind Tafjord, Peter Clark, and Ashwin Kalyan. Learn to explain: Multimodal reasoning via thought chains for science question answering. *Advances in Neural Information Processing Systems*, 35:2507–2521, 2022. 2, 7

[27] Pan Lu, Hritik Bansal, Tony Xia, Jiacheng Liu, Chunyuan Li, Hannaneh Hajishirzi, Hao Cheng, Kai-Wei Chang, Michel Galley, and Jianfeng Gao. Mathvista: Evaluating mathematical reasoning of foundation models in visual contexts. *arXiv preprint arXiv:2310.02255*, 2023. 2, 7

[28] Xueguang Ma, Qian Liu, Dongfu Jiang, Ge Zhang, Zejun Ma, and Wenhu Chen. General-reasoner: Advancing llm reasoning across all domains. *arXiv preprint arXiv:2505.14652*, 2025. 2

[29] Ahmed Masry, Xuan Long Do, Jia Qing Tan, Shafiq Joty, and Enamul Hoque. Chartqa: A benchmark for question answering about charts with visual and logical reasoning. In *Findings of the association for computational linguistics: ACL 2022*, pages 2263–2279, 2022. 2, 7

[30] Minesh Mathew, Dimosthenis Karatzas, and CV Jawahar. Docvqa: A dataset for vqa on document images. In *Proceedings of the IEEE/CVF winter conference on applications of computer vision*, pages 2200–2209, 2021. 1, 7

[31] Minesh Mathew, Viraj Bagal, Rubèn Tito, Dimosthenis Karatzas, Ernest Valveny, and CV Jawahar. Infographicvqa. In *Proceedings of the IEEE/CVF Winter Conference on Applications of Computer Vision*, pages 1697–1706, 2022. 1, 2, 7

[32] Grégoire Mialon, Clémentine Fourrier, Thomas Wolf, Yann LeCun, and Thomas Scialom. Gaia: a benchmark for general ai assistants. In *The Twelfth International Conference on Learning Representations*, 2023. 1

[33] Long Ouyang, Jeffrey Wu, Xu Jiang, Diogo Almeida, Carroll Wainwright, Pamela Mishkin, Chong Zhang, Sandhini Agarwal, Katarina Slama, Alex Ray, et al. Training language models to follow instructions with human feedback. *Advances in neural information processing systems*, 35:27730–27744, 2022. 1, 2

[34] Rafael Rafailov, Archit Sharma, Eric Mitchell, Christopher D Manning, Stefano Ermon, and Chelsea Finn. Direct preference optimization: Your language model is secretly a reward model. *Advances in neural information processing systems*, 36:53728–53741, 2023. 1

[35] Dustin Schwenk, Apoorv Khandelwal, Christopher Clark, Kenneth Marino, and Roozbeh Mottaghi. A-okvqa: A benchmark for visual question answering using world knowledge. In *European conference on computer vision*, pages 146–162. Springer, 2022. 2, 7

[36] Zhihong Shao, Peiyi Wang, Qihao Zhu, Runxin Xu, Junxiao Song, Xiao Bi, Haowei Zhang, Mingchuan Zhang, YK Li, Yang Wu, et al. Deepseekmath: Pushing the limits of mathematical reasoning in open language models. *arXiv preprint arXiv:2402.03300*, 2024. 2, 3

[37] Yi Su, Dian Yu, Linfeng Song, Juntao Li, Haitao Mi, Zhaopeng Tu, Min Zhang, and Dong Yu. Crossing the reward bridge: Expanding rl with verifiable rewards across diverse domains. *arXiv preprint arXiv:2503.23829*, 2025. 1

[38] Zhenwei Tang, Difan Jiao, Blair Yang, and Ashton Anderson. Seam: Semantically equivalent across modalities benchmark for vision-language models. *arXiv preprint arXiv:2508.18179*, 2025. 2

[39] Gemma Team, Thomas Mesnard, Cassidy Hardin, Robert Dadashi, Surya Bhupatiraju, Shreya Pathak, Laurent Sifre, Morgane Rivière, Mihir Sanjay Kale, Juliette Love, et al. Gemma: Open models based on gemini research and technology. *arXiv preprint arXiv:2403.08295*, 2024. 2

[40] Hugo Touvron, Thibaut Lavril, Gautier Izacard, Xavier Martinet, Marie-Anne Lachaux, Timothée Lacroix, Baptiste Rozière, Naman Goyal, Eric Hambro, Faisal Azhar, et al. Llama: Open and efficient foundation language models. *arXiv preprint arXiv:2302.13971*, 2023. 2

[41] Tao Tu, Anil Palepu, Mike Schaekermann, Khaled Saab, Jan Freyberg, Ryutaro Tanno, Amy Wang, Brenna Li, Mohamed Amin, Nenad Tomasev, et al. Towards conversational diagnostic ai. *arXiv preprint arXiv:2401.05654*, 2024. 2

[42] Wenhai Wang, Zhe Chen, Xiaokang Chen, Jiannan Wu, Xizhou Zhu, Gang Zeng, Ping Luo, Tong Lu, Jie Zhou, Yu Qiao, et al. Visionllm: Large language model is also an open-ended decoder for vision-centric tasks. *Advances in Neural Information Processing Systems*, 36:61501–61513, 2023. 2

[43] Weiqin Wang, Yile Wang, and Hui Huang. Ranked voting based self-consistency of large language models. *arXiv preprint arXiv:2505.10772*, 2025. 1

[44] Xuezhi Wang, Jason Wei, Dale Schuurmans, Quoc Le, Ed Chi, Sharan Narang, Aakanksha Chowdhery, and Denny Zhou. Self-consistency improves chain of thought reasoning in language models. *arXiv preprint arXiv:2203.11171*, 2022. 1

[45] Yizhong Wang, Yeganeh Kordi, Swaroop Mishra, Alisa Liu, Noah A Smith, Daniel Khashabi, and Hannaneh Hajishirzi. Self-instruct: Aligning language models with self-generated instructions. *arXiv preprint arXiv:2212.10560*, 2022. 1, 2

[46] Jason Wei, Xuezhi Wang, Dale Schuurmans, Maarten Bosma, Fei Xia, Ed Chi, Quoc V Le, Denny Zhou, et al. Chain-of-thought prompting elicits reasoning in large language models. *Advances in neural information processing systems*, 35:24824–24837, 2022. 2

[47] Xumeng Wen, Zihan Liu, Shun Zheng, Shengyu Ye, Zhirong Wu, Yang Wang, Zhijian Xu, Xiao Liang, Junjie Li, Ziming Miao, et al. Reinforcement learning with verifiable rewards implicitly incentivizes correct reasoning in base llms. *arXiv preprint arXiv:2506.14245*, 2025. 1, 2

[48] Tianbao Xie, Danyang Zhang, Jixuan Chen, Xiaochuan Li, Siheng Zhao, Ruisheng Cao, Toh J Hua, Zhoujun Cheng, Dongchan Shin, Fangyu Lei, et al. Osworld: Benchmarking multimodal agents for open-ended tasks in real computer environments. *Advances in Neural Information Processing Systems*, 37:52040–52094, 2024. 1

[49] Yifei Xu, Tusher Chakraborty, Srinagesh Sharma, Leonardo Nunes, Emre Kıcıman, Songwu Lu, and Ranveer Chandra. Direct reasoning optimization: Llms can reward and refine their own reasoning for open-ended tasks. *arXiv preprint arXiv:2506.13351*, 2025. 2

[50] An Yang, Anfeng Li, Baosong Yang, Beichen Zhang, Binyuan Hui, Bo Zheng, Bowen Yu, Chang Gao, Chengen Huang, Chenxu Lv, et al. Qwen3 technical report. *arXiv preprint arXiv:2505.09388*, 2025. 2

[51] Zhengyuan Yang, Linjie Li, Jianfeng Wang, Kevin Lin, Ehsan Azarnasab, Faisal Ahmed, Zicheng Liu, Ce Liu, Michael Zeng, and Lijuan Wang. Mm-react: Prompting chatgpt for multimodal reasoning and action. *arXiv preprint arXiv:2303.11381*, 2023. 1

[52] Fan Yuan, Yuchen Yan, Yifan Jiang, Haoran Zhao, Tao Feng, Jinyan Chen, Yanwei Lou, Wenqi Zhang, Yongliang Shen, Weiming Lu, et al. Gsm8k-v: Can vision language models solve grade school math word problems in visual contexts. *arXiv preprint arXiv:2509.25160*, 2025. 2

[53] Weizhe Yuan, Richard Yuanzhe Pang, Kyunghyun Cho, Sainbayar Sukhbaatar, Jing Xu, and Jason Weston. Self-rewarding language models. *arXiv preprint arXiv:2401.10020*, 3, 2024. 2

[54] Eric Zelikman, Yuhuai Wu, Jesse Mu, and Noah D Goodman. Star: Self-taught reasoner bootstrapping reasoning with reasoning. In *Proc. the 36th International Conference on Neural Information Processing Systems*, 2024. 1

[55] Kongcheng Zhang, Qi Yao, Shunyu Liu, Yingjie Wang, Baisheng Lai, Jieping Ye, Mingli Song, and Dacheng Tao. Consistent paths lead to truth: Self-rewarding reinforcement learning for llm reasoning. *arXiv preprint arXiv:2506.08745*, 2025. 2

[56] Renrui Zhang, Jiaming Han, Chris Liu, Peng Gao, Aojun Zhou, Xiangfei Hu, Shilin Yan, Pan Lu, Hongsheng Li, and Yu Qiao. Llama-adapter: Efficient fine-tuning of language models with zero-init attention. *arXiv preprint arXiv:2303.16199*, 2023. 2

[57] Tinghui Zhu, Qin Liu, Fei Wang, Zhengzhong Tu, and Muhao Chen. Unraveling cross-modality knowledge conflicts in large vision-language models. *arXiv preprint arXiv:2410.03659*, 2024. 1, 2

[58] Mingchen Zhuge, Changsheng Zhao, Dylan Ashley, Wenyi Wang, Dmitrii Khizbullin, Yunyang Xiong, Zechun Liu, Ernie Chang, Raghuraman Krishnamoorthi, Yuandong Tian, et al. Agent-as-a-judge: Evaluate agents with agents. *arXiv preprint arXiv:2410.10934*, 2024. 2

[59] Yuxin Zuo, Kaiyan Zhang, Li Sheng, Shang Qu, Ganqu Cui, Xuekai Zhu, Haozhan Li, Yuchen Zhang, Xinwei Long, Ermo Hua, et al. Ttrl: Test-time reinforcement learning. *arXiv preprint arXiv:2504.16084*, 2025. 2

R-C^2: Cross-Modal Cycle Consistency Rewards Improve Multimodal Reasoning

Supplementary Material

A. Training Hyperparameters

The key global hyperparameters used throughout all experiments in this paper are listed in Table A1. Unless explicitly stated otherwise, all models were trained under this shared configuration.

Parameter	**Value**
Global Batch Size	(256, 1024)
Learning Rate	1×10^{-6}
Weight Decay	1×10^{-2}
KL Penalty Coefficient (λ_{KL})	1×10^{-2}
Max Steps	100
Number of Rollouts	4
Temperature	1.0
Top-p	0.95

Table A1. Key global hyperparameters used throughout our experiments. Larger batch sizes are adopted when GPU memory permits.

B. Reproposed VWA Task

To enable a more straightforward evaluation of multimodal web understanding, we redesign the VWA dataset into a multiple-choice question answering (MC-QA) task based on shopping-website pages. For each webpage, we automatically generate question–answer pairs using GPT-5, followed by human verification to ensure correctness and quality. Each page contains **10** questions, and each question provides **6** candidate choices, with **1** correct answer. Visualized examples are provided in Figures 8 and 9.

C. Prompt Templates

We list the prompt templates used during training and evaluation in Table A3.

Figure 8. Examples from the repurposed VWA multiple-choice dataset constructed on shopping webpages. For each webpage, we generate **10** questions with **6** answer choices, among which **1** is correct. The questions cover diverse reasoning types, including product category recognition, price comparison, customer rating analysis, and attribute identification.

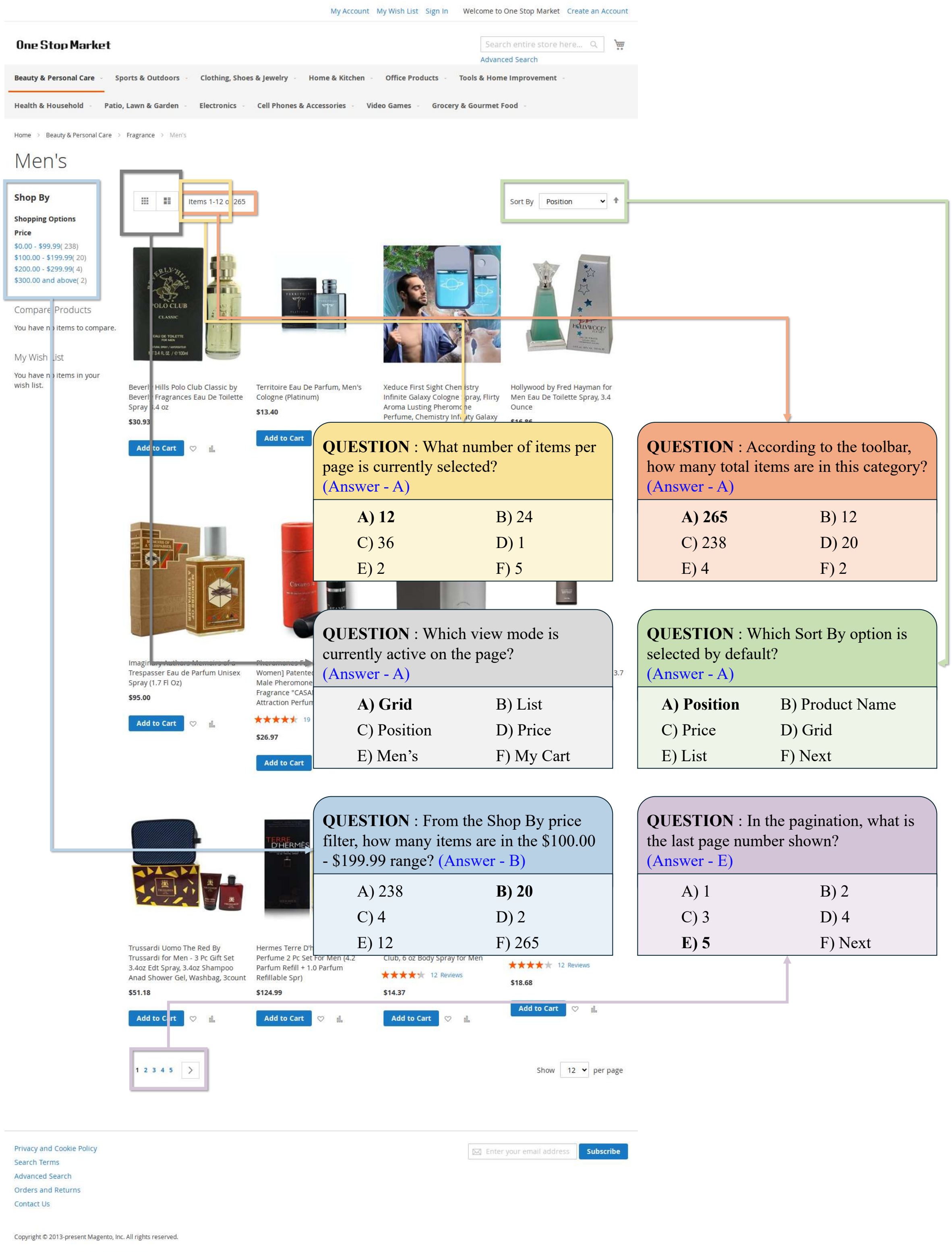

Figure 9. Examples from the repurposed VWA multiple-choice dataset constructed on shopping webpages.

Dataset	Prompt Template
DocVQA & InfoVQA	BACKWARD QUERY GENERATION **System Message:** You are a question generator. Given an observation of a document (infographic) and the correct Answer, produce a single, concise, unambiguous question whose answer is exactly the given Answer and should be asking about the information provided by the observation; when grounded ONLY on the observation provided. Rules: (1) Return ONLY the question text. (2) Avoid ambiguous wording; ensure a 1-to-1 mapping, this means the query should not have answers to it other than the correct Answer provided to you. (3) No extra commentary, quotes, or prefixes. (4) Make sure that the question is asking about the observed document (infographic), don't propose random answers to fit the answer. **User Message:** Base rule: You need to generate a question. Here is the structure of the examples: *few shot examples:* Example i OBS: `[TEXT_OBS]` or `[IMAGE_OBS]` Answer: `[ANS]` Given the observation of the document (infographic), I will come up with a document (infographic) facts based Query that can be answered by the given answer. Query is: `[QUESTION]` *The remaining examples follow the same structure.* Visual focus: In this task, the OBS is an image version of the document (infographic). You must generate the question based solely on visible information in the image, without assuming or inferring any unseen text or external knowledge. Textual focus: In this task, the OBS is ocr and captioning of an document (infographic) image. OBS: `[TEXT_OBS]` or `[IMAGE_OBS]` Answer: `[ANS]` Given the observation of the document (infographic), I will come up with a document (infographic) facts based Query that can be answered by the given answer. Query is: **Assistant Message:** (Generated response)
	CYCLE VERIFICATION **User Message:** You are a helpful assistant for document VQA. Answer with the exact final answer only. OBS: `[TEXT_OBS]` or `[IMAGE_OBS]` Query: `[QUESTION]` Answer concisely with only the final answer. **Assistant Message:** (Generated response)

Table A2. **Prompt templates for each dataset and prompt type.** The BACKWARD QUERY GENERATION prompt infers plausible multimodal queries conditioned on each candidate answer; and the CYCLE VERIFICATION prompt assesses whether forward inference from these queries reconstructs the original answer, providing the cycle-consistency supervision signal.

Dataset	Prompt Template
ChartQA	BACKWARD QUERY GENERATION **Image-specific part:** [IMAGE_OBS] You are writing ONE short, clear, self-contained question about a chart image such that the answer equals a GIVEN TARGET ANSWER. **Text-specific part:** You are writing ONE short, clear, self-contained question about a chart based ONLY on the following caption text. The question must have the GIVEN TARGET ANSWER. [TEXT_OBS]: **Shared rules and ending:** Rules: - Must be answerable using chart visual information only. - Must not reveal or restate the answer. - Avoid yes/no, multiple choice, multi-part questions. - Include necessary qualifiers (series, category, unit, timestamp). - Length: 1–2 sentences, no explanation. Target Answer: [ANSWER]. Write the question now. Return only the question string.
	CYCLE VERIFICATION **Image-based QA Prompt:** [IMAGE_OBS] You are given a chart image and a question. Use ONLY the information that is explicitly visible in the chart (titles, labels, legends, tick marks, data labels, notes). Question: [QUESTION] Answer concisely with plain or numeric text only (no reasoning, no steps, no formatting). **Text-based QA Prompt:** You are given a chart description in JSON extracted from an image. Answer the user's question using ONLY the information contained in the JSON. JSON: [TEXT_OBS] Question: [QUESTION] Answer concisely with plain or numeric text only (no reasoning, no steps, no formatting).

Table A3. **Prompt templates for each dataset and prompt type.** The BACKWARD QUERY GENERATION prompt infers plausible multimodal queries conditioned on each candidate answer; and the CYCLE VERIFICATION prompt assesses whether forward inference from these queries reconstructs the original answer, providing the cycle-consistency supervision signal.